Structural Engineering and Mechanics, *Vol. 75, No. 6 (2020) 701-711*
DOI: https://doi.org/10.12989/sem.2020.75.6.701

Porosity effects on post-buckling behavior of geometrically imperfect metal foam doubly-curved shells with stiffeners

Seyed Sajad Mirjavadi[1], Masoud Forsat*[1], Yahya Zakariya Yahya[2], Mohammad Reza Barati[3], Anirudh Narasimamurthy Jayasimha[4] and AMS Hamouda[1]

[1]*Department of Mechanical and Industrial Engineering, Qatar University, P.O. Box 2713, Doha, Qatar*
[2]*Auckland Bioengineering Institute, the University of Auckland, Auckland, New Zealand*
[3]*Fidar project Qaem Company, Darvazeh Dolat, Tehran, Iran*
[4]*Bonn-Rhein-Sieg University of Applied Science, Sankt Augustin, Germany*

(Received February 9, 2020, Revised March 1, 2020, Accepted April 14, 2020)

Abstract. This papers studies nonlinear stability and post-buckling behaviors of geometrically imperfect metal foam doubly-curved shells with eccentrically stiffeners resting on elastic foundation. Metal foam is considered as porous material with uniform and non-uniform models. The doubly-curved porous shell is subjected to in-plane compressive loads as well as a transverse pressure leading to post-critical stability in nonlinear regime. The nonlinear governing equations are analytically solved with the help of Airy stress function to obtain the post-buckling load-deflection curves of the geometrically imperfect metal foam doubly-curved shell. Obtained results indicate the significance of porosity distribution, geometrical imperfection, foundation factors, stiffeners and geometrical parameters on post-buckling characteristics of porous doubly-curved shells.

Keywords: post-buckling; shell theory; porous material; curved shell; nonlinear stability; stiffeners

1. Introduction

Metal foams are in the category of porous materials with low weight due to possessing different variations of porosities in them (Ahmed *et al*. 2019, Al-Maliki *et al*. 2019). Applying mechanical loads to such material structures yields elastic deformations and changed vibrational properties (Shafiei *et al*. 2017, Mirjavadi *et al*. 2017&2018&2019, Azimi *et al*. 2017,2018). The variation of porosities in this material causes a significant difference between metal foams and other perfect metals. In a non-perfect metal, the material characteristics are notably influenced by pore variations. Also, this variation in pores can affect the vibration frequencies of engineering structures made of metal foams. This issue can be understood from the works done by Chen *et al*. 2015 and 2016. Different from metal foams, there are also functionally graded (FG) or ceramic-metal materials in which pore variation effect is very important (Abdelaziz *et al*. 2017, Zarga *et al*. 2019, Zine *et al*. 2018, Yahiaoui *et al*. 2018, Medani *et al*. 2019, Meksi *et al*. 2019, Mahmoudi *et al*. 2019, Achouri *et al*. 2019). In this material, pores may be produced in a phase between ceramic and material (Attia *et al*. 2018, Addou *et al*. 2019). Engineering structures made of this materials are studied to understand their vibration behaviors as reported in the works of Wattanasakulpong *et al*. (2014), Atmane *et al*. 2015). This type of material is used in different structures such as beams, plates and shells (Bellifa *et al*. 2017, Boukhlif *et al*. 2019). There are some studies on different structures in the literature (Berrabah *et al*. 2013, Aissani *et al*. 2015, Sahu *et al*. 2018, Nebab *et al*. 2019).

Curved shell structures with single or double curvatures are a particular sort of modern structures, frequently applied in the industries like aero-space, aircrafts, space vehicles, space engineering and in other serious engineering fields. The study of static and dynamic behaviors of such structures is essential to have impressive and reliable designs. Recently, some authors studied mechanical behaviors of doubly-curved shells made of different materials. Zare Jouneghani *et al*. (2017) examined linear vibration properties of FG double-curve shells based on porosity effects. Zhao *et al*. (2019) examined linear vibrations of porous FG shells with considering general types of boundary conditions. Also, Li *et al*. (2019) provided a numerical solution for free vibrations of FG shells with double curvatures and non-uniform thickness. Trinh *et al*. (2019) explored the temperature and porosity impacts on free vibration characteristics of FG double-curve shells.

All of above mentioned articles related to porous doubly-curved shells neglects the influences of geometrical imperfection and stiffeners. Geometry imperfections are created during operation life or set up of curved shells and result in changed mechanical properties (Barati and Zenkour 2018). Stiffened plates and shells are sorts of structures fortified via arrays of stiffeners for enhancing their loads carrying capacity, and broadly applied in modern engineering nowadays. Accordingly, there have been many studies on the stability and dynamics of stiffened structures (Duc *et al*. 2016). Based on above discussion, nonlinear

*Corresponding author, Professor
E-mail: masoudforsatlar@gmail.com

ISSN: 1225-4568 (Print), 1598-6217 (Online)

stability analysis of geometrically imperfect and stiffened doubly-curved porous shells under mechanical loads is not performed yet.

The present article is devoted to analyze nonlinear stability and post-buckling behavior of a geometrically imperfect doubly-curved shell made of porous metal foam under compressive loads and lateral pressure. The formulation of doubly-curved shell is based on classic thin shell theory. Porosities have two types of dispersion within the structure including uniform and non-uniform. The nonlinear governing equations are analytically solved with the help of Airy stress function to obtain the post-buckling load-deflection curves of the geometrically imperfect metal foam doubly-curved shell. Obtained results indicate the significance of porosity distribution, geometrical imperfection, foundation factors, stiffeners and geometrical parameters on post-buckling characteristics of porous doubly-curved shells.

2. Porous metal foam material with open cells

A porous material, for instance a steel foam, might be placed in the category of lightweight materials and can be applied in several structures such as curved panels. Often, pore variation along the thickness of shells results in a notable alteration in every kind of material property. When the pore distribution inside the material is selected to be non-uniform, the metal foam might be defined as a functionally graded material since its properties obey some specified functions. Herein, the following types of pore dispersion will be employed (Ahmed *et al*. 2019, Fenjan *et al*. 2019):

- Uniform kind

$$E = E_2(1-e_0\chi) \tag{1a}$$

$$G = G_2(1-e_0\chi) \tag{1b}$$

$$\rho = \rho_2\sqrt{(1-e_0\chi)} \tag{1c}$$

- Non-uniform kind

$$E(z) = E_2(1-e_0\cos\left(\frac{\pi z}{h}\right)) \tag{2a}$$

$$G(z) = G_2(1-e_0\cos\left(\frac{\pi z}{h}\right)) \tag{2b}$$

$$\rho(z) = \rho_2(1-e_m\cos\left(\frac{\pi z}{h}\right)) \tag{2c}$$

The most important factors in above relations are the greatest values of material properties E_2, G_2 and ρ_2. Also, there are two important factors related to pores and mass which are e_0 and e_m as:

$$e_0 = 1-\frac{E_2}{E_1} = 1-\frac{G_2}{G_1}, e_m = 1-\frac{\rho_2}{\rho_1} = 1-\sqrt{1-e_0} \tag{3}$$

Based on the open cell assumption of porous material, we use the following relations:

$$\frac{E_2}{E_1} = \left(\frac{\rho_2}{\rho_1}\right)^2 \tag{4}$$

Based on uniformly distributed pores, the following parameter is used in Eq.(1) as:

$$\chi = \frac{1}{e_0} - \frac{1}{e_0}\left(\frac{2}{\pi}\sqrt{1-e_0} - \frac{2}{\pi} + 1\right)^2 \tag{5}$$

3. Governing equations

So far, a variety of plate-shell theories are introduced for description and analyzes of the structures (Abualnour *et al*. 2019, Tounsi *et al*. 2020, Asghar *et al*. 2020, Adda Bedia *et al*. 2019, Alimirzaei *et al*. 2019, Batou *et al*. 2019, Belbachir *et al*. 2019, Berghouti *et al*. 2019, Boukhlif *et al*. 2019, Bourada *et al*. 2019, Boutaleb *et al*. 2019, Boulefrakh *et al*. 2019, Chaabane *et al*. 2019, Draoui *et al*. 2019, Hellal *et al*. 2019, Hussain *et al*. 2019, Kaddari *et al*. 2020, Khiloun *et al*. 2019, Sahla *et al*. 2019, Semmah *et al*. 2019, Tlidji *et al*. 2019, Zarga *et al*. 2019, Zaoui *et al*. 2019). In this article, classic shell theory has been employed for mathematical modeling of the doubly-curved shells. Thus, the strain field can be introduced by (Duc and Quan 2014):

$$\begin{Bmatrix}\varepsilon_x\\ \varepsilon_y\\ \gamma_{xy}\end{Bmatrix} = \begin{Bmatrix}\varepsilon_x^0\\ \varepsilon_y^0\\ \gamma_{xy}^0\end{Bmatrix} + z\begin{Bmatrix}k_x\\ k_y\\ 2k_{xy}\end{Bmatrix} \tag{6}$$

in which

$$\begin{aligned}
&\varepsilon_x^0 = \frac{\partial u}{\partial x} + \frac{1}{2}(\frac{\partial w}{\partial x})^2 - \frac{w}{R_x},\\
&\varepsilon_y^0 = \frac{\partial v}{\partial y} + \frac{1}{2}(\frac{\partial w}{\partial y})^2 - \frac{w}{R_y},\\
&\gamma_{xy}^0 = \frac{\partial u}{\partial y} + \frac{\partial v}{\partial x} + \frac{\partial w}{\partial x}\frac{\partial w}{\partial y},\\
&k_x = -\frac{\partial^2 w}{\partial x^2},\ k_y = -\frac{\partial^2 w}{\partial y^2},\ k_{xy} = -\frac{\partial^2 w}{\partial x \partial y}
\end{aligned} \tag{7}$$

The presented field contains transverse (w) and in-plane (u, v) components. Based on the classic shell assumption, stress-strain relations can be summarized as (Ahmed *et al*. 2019):

$$\begin{Bmatrix}\sigma_x\\ \sigma_y\\ \sigma_{xy}\end{Bmatrix}=\frac{E(z)}{1-\nu^2}\begin{pmatrix}1 & \nu & 0\\ \nu & 1 & 0\\ 0 & 0 & (1-\nu)/2\end{pmatrix}\begin{Bmatrix}\varepsilon_x\\ \varepsilon_y\\ \gamma_{xy}\end{Bmatrix} \quad (8)$$

where σ_i (i=x, y, xy) are stress field components. The stresses leads to below resultants via integrating Eq.(8) over shell thickness as:

$$N_x=(A_{10}+\frac{E_sA_{sx}}{s_x})\varepsilon_x^0+A_{20}\varepsilon_y^0+(A_{11}+C_x)k_x+A_{21}k_y \quad (9)$$

$$N_y=A_{20}\varepsilon_x^0+(A_{10}+\frac{E_sA_{sy}}{s_y})\varepsilon_y^0+A_{21}k_x+(A_{11}+C_y)k_y \quad (10)$$

$$N_{xy}=A_{30}\gamma_{xy}^0+2A_{31}k_{xy} \quad (11)$$

$$M_x=(A_{11}+C_x)\varepsilon_x^0+A_{21}\varepsilon_y^0+(A_{12}+\frac{E_sI_{sx}}{s_x})k_x+A_{22}k_y \quad (12)$$

$$M_y=A_{21}\varepsilon_x^0+(A_{11}+C_y)\varepsilon_y^0+A_{22}k_x+(A_{12}+\frac{E_sI_{sy}}{s_y})k_y \quad (13)$$

$$M_{xy}=A_{31}\gamma_{xy}^0+2A_{32}k_{xy} \quad (14)$$

in which E_s is Young's modulus of stiffeners; s_x nd s_y are spacing of longitudinal and lateral stiffeners; A_{sx} and A_{sy} are cross sections of stiffeners and

$$\begin{aligned}&A_{10}=\int_{-h/2}^{h/2}\frac{E(z)}{1-\nu^2}dz,\ A_{11}=\int_{-h/2}^{h/2}\frac{E(z)}{1-\nu^2}zdz,A_{12}=\int_{-h/2}^{h/2}\frac{E(z)}{1-\nu^2}z^2dz\\ &A_{20}=\int_{-h/2}^{h/2}\frac{E(z)\nu}{1-\nu^2}dz,\ A_{21}=\int_{-h/2}^{h/2}\frac{E(z)\nu}{1-\nu^2}zdz,A_{22}=\int_{-h/2}^{h/2}\frac{E(z)\nu}{1-\nu^2}z^2dz\\ &A_{30}=\int_{-h/2}^{h/2}\frac{E(z)}{2(1+\nu)}dz,\ A_{31}=\int_{-h/2}^{h/2}\frac{E(z)}{2(1+\nu)}zdz,A_{32}=\int_{-h/2}^{h/2}\frac{E(z)}{2(1+\nu)}z^2dz\end{aligned} \quad (15)$$

And

$$\begin{aligned}&I_{sx}=\frac{b_x\left(h_x\right)^3}{12}+A_{sx}\left(z_x\right)^2,\quad I_{sy}=\frac{b_y\left(h_y\right)^3}{12}+A_{sy}\left(z_y\right)^2\\ &C_x=\frac{E_sA_{sx}z_x}{s_x},\quad C_y=\frac{E_sA_{sy}z_y}{s_y}\\ &z_x=0.5(h+h_x),\quad z_y=0.5(h+h_y)\end{aligned} \quad (16)$$

Note that h_x and h_y are height of stiffeners; b_x and b_y are width of stiffeners. The well-known governing equations for a doubly-curved shells under transverse pressure (q) may be expressed by:

$$\frac{\partial N_x}{\partial x}+\frac{\partial N_{xy}}{\partial y}=0 \quad (17)$$

$$\frac{\partial N_{xy}}{\partial x}+\frac{\partial N_y}{\partial y}=0 \quad (18)$$

$$\begin{aligned}&\frac{\partial^2M_x}{\partial x^2}+2\frac{\partial^2M_{xy}}{\partial x\partial y}+\frac{\partial^2M_y}{\partial y^2}+\frac{N_x}{R_x}+\frac{N_y}{R_y}+N_x\frac{\partial^2w}{\partial x^2}+2N_{xy}\frac{\partial^2w}{\partial x\partial y}+N_y\frac{\partial^2w}{\partial y^2}\\ &-k_ww+k_P(\frac{\partial^2w}{\partial x^2}+\frac{\partial^2w}{\partial y^2})=q\end{aligned} \quad (19)$$

in which k_W and k_p are linear and shear foundation parameters. Now, using Eqs. (9)-(14), it is possible to obtain in-plane strains as:

$$\begin{aligned}\varepsilon_x^0&=\tilde{A}_{22}N_x-\tilde{A}_{12}N_y+B_{11}\frac{\partial^2w}{\partial x^2}+B_{12}\frac{\partial^2w}{\partial y^2}\\ \varepsilon_y^0&=\tilde{A}_{11}N_y-\tilde{A}_{12}N_x+B_{21}\frac{\partial^2w}{\partial x^2}+B_{22}\frac{\partial^2w}{\partial y^2}\\ \gamma_{xy}^0&=\tilde{A}_{66}N_{xy}+2B_{66}\frac{\partial^2w}{\partial x\partial y}\end{aligned} \quad (20)$$

in which

$$\begin{aligned}\tilde{A}_{11}&=\frac{1}{(A_{10}+\frac{E_sA_{sx}}{s_x})(A_{10}+\frac{E_sA_{sy}}{s_y})-A_{20}^2}(A_{10}+\frac{E_sA_{sx}}{s_x})\\ \tilde{A}_{22}&=\frac{1}{(A_{10}+\frac{E_sA_{sx}}{s_x})(A_{10}+\frac{E_sA_{sy}}{s_y})-A_{20}^2}(A_{10}+\frac{E_sA_{sy}}{s_y})\\ \tilde{A}_{12}&=\frac{A_{20}}{(A_{10}+\frac{E_sA_{sx}}{s_x})(A_{10}+\frac{E_sA_{sy}}{s_y})-A_{20}^2}\\ B_{11}&=\tilde{A}_{22}(A_{11}+C_x)-\tilde{A}_{12}A_{21}\\ B_{22}&=\tilde{A}_{11}(A_{11}+C_y)-\tilde{A}_{12}A_{21}\\ B_{12}&=\tilde{A}_{22}A_{21}-\tilde{A}_{12}(A_{11}+C_y)\\ B_{21}&=\tilde{A}_{11}A_{21}-\tilde{A}_{12}(A_{11}+C_x)\\ \tilde{A}_{66}&=\frac{1}{A_{30}},\quad B_{66}=\frac{A_{31}}{A_{30}}\end{aligned} \quad (21)$$

Now, the Airy stress function (F) can be introduced by:

$$\frac{\partial^2F}{\partial y^2}=N_x,\ \frac{\partial^2F}{\partial x\partial y}=-N_{xy},\ \frac{\partial^2F}{\partial x^2}=N_y \quad (22)$$

By using above definitions and considering geometric imperfection deflection (w^*), the governing equation becomes:

$$\begin{aligned}&B_{21}\frac{\partial^4F}{\partial x^4}+B_{12}\frac{\partial^4F}{\partial y^4}+(B_{11}+B_{22}-2B_{66})\frac{\partial^4F}{\partial x^2\partial y^2}-D_{11}\frac{\partial^4w}{\partial x^4}-D_{22}\frac{\partial^4w}{\partial y^4}\\ &-(D_{12}+D_{21}+4D_{66})\frac{\partial^4w}{\partial x^2\partial y^2}+\frac{\partial^2F}{\partial y^2}(\frac{\partial^2w}{\partial x^2}+\frac{\partial^2w^*}{\partial x^2})-2\frac{\partial^2F}{\partial x\partial y}(\frac{\partial^2w}{\partial x\partial y}+\frac{\partial^2w^*}{\partial x\partial y})\\ &+\frac{\partial^2F}{\partial x^2}(\frac{\partial^2w}{\partial y^2}+\frac{\partial^2w^*}{\partial y^2})+\frac{1}{R_x}\frac{\partial^2F}{\partial y^2}+\frac{1}{R_y}\frac{\partial^2F}{\partial x^2}-k_ww+k_P(\frac{\partial^2w}{\partial x^2}+\frac{\partial^2w}{\partial y^2})=q\end{aligned} \quad (23)$$

The compatibility equation for a double-curve shell having geometric imperfectness might be denoted as:

$$\begin{aligned}&\frac{\partial^2\varepsilon_x^0}{\partial y^2}+\frac{\partial^2\varepsilon_y^0}{\partial x^2}-\frac{\partial^2\gamma_{xy}^0}{\partial x\partial y}\\ &=\left(\frac{\partial^2w}{\partial x\partial y}\right)^2-\frac{\partial^2w}{\partial x^2}\frac{\partial^2w}{\partial y^2}+2\frac{\partial^2w}{\partial x\partial y}\frac{\partial^2w^*}{\partial x\partial y}-\frac{\partial^2w}{\partial x^2}\frac{\partial^2w^*}{\partial y^2}\\ &-\frac{\partial^2w}{\partial y^2}\frac{\partial^2w^*}{\partial x^2}-\frac{1}{R_x}\frac{\partial^2w}{\partial y^2}-\frac{1}{R_y}\frac{\partial^2w}{\partial x^2}\end{aligned} \quad (24)$$

Now, Eq.(20) can be expressed in terms of stress function (F) as:

$$\varepsilon_x^0 = \tilde{A}_{22}\frac{\partial^2 F}{\partial y^2} - \tilde{A}_{12}\frac{\partial^2 F}{\partial x^2} + B_{11}\frac{\partial^2 w}{\partial x^2} + B_{12}\frac{\partial^2 w}{\partial y^2}$$
$$\varepsilon_y^0 = \tilde{A}_{11}\frac{\partial^2 F}{\partial x^2} - \tilde{A}_{12}\frac{\partial^2 F}{\partial y^2} + B_{21}\frac{\partial^2 w}{\partial x^2} + B_{22}\frac{\partial^2 w}{\partial y^2} \quad (25)$$
$$\gamma_{xy}^0 = -\tilde{A}_{66}\frac{\partial^2 F}{\partial x \partial y} + 2B_{66}\frac{\partial^2 w}{\partial x \partial y}$$

Placing Eq. (20) in Eq. (24) results in the compatibility equation of an imperfect metal foam doubly curved shells as:

$$\tilde{A}_{11}\frac{\partial^4 F}{\partial x^4} + \tilde{A}_{22}\frac{\partial^4 F}{\partial y^4} + (\tilde{A}_{66} - 2\tilde{A}_{12})\frac{\partial^4 F}{\partial x^2 \partial y^2}$$
$$+B_{21}\frac{\partial^4 w}{\partial x^4} + B_{12}\frac{\partial^4 w}{\partial y^4} + (B_{11} + B_{22} - 2B_{66})\frac{\partial^4 w}{\partial x^2 \partial y^2}$$
$$= \left(\frac{\partial^2 w}{\partial x \partial y}\right)^2 - \frac{\partial^2 w}{\partial x^2}\frac{\partial^2 w}{\partial y^2} + 2\frac{\partial^2 w}{\partial x \partial y}\frac{\partial^2 w^*}{\partial x \partial y} - \frac{\partial^2 w}{\partial x^2}\frac{\partial^2 w^*}{\partial y^2} \quad (26)$$
$$-\frac{\partial^2 w}{\partial y^2}\frac{\partial^2 w^*}{\partial x^2} - \frac{1}{R_x}\frac{\partial^2 w}{\partial y^2} - \frac{1}{R_y}\frac{\partial^2 w}{\partial x^2}$$

The above equation must be solved together with Eq. (23) to obtain post-buckling path of the present shell model.

4. Method of solution

According to the section, the solution of the nonlinear governing equations for the post-buckling of a metal foam doubly-curved shell has been represented. For the mechanical post-buckling study of simply-supported shells, the freely moving edge conditions are:

$$w = N_{xy} = M_x = \frac{\partial^2 F}{\partial x \partial y} = 0, \qquad \int_0^b \frac{\partial^2 F}{\partial y^2} dy = -P_x h \quad (27)$$

at x=0,a

$$w = N_{xy} = M_y = \frac{\partial^2 F}{\partial x \partial y} = 0, \qquad \int_0^a \frac{\partial^2 F}{\partial x^2} dx = -P_y h \quad (28)$$

at y=0,b

Then, the displacements are considered in the following form:

$$w = \sum_{m=1}^{\infty}\sum_{n=1}^{\infty} \tilde{W} f_m^w(x) g_n^w(y) \quad (29)$$

$$w^* = \sum_{m=1}^{\infty}\sum_{n=1}^{\infty} W^* f_m^{w*}(x) g_n^{w*}(y) \quad (30)$$

where $\tilde{W}$ and W^* are the deflection amplitude and imperfection amplitude, respectively. For simply-supported edges let $f_m^w = f_m^{w*} = sin(\lambda_m x)$ with $\lambda_m = m\pi/a$ and $g_n^w = g_n^{w*}(y) = sin(\delta_n y)$ with $\delta_n = n\pi/b$. Via employment of the edge conditions in Eqs.(27)-(28) and displacement components in Eq.(29)-(30), the general expression for stress function F may be introduced by:

$$F = \Phi_1 \cos(2\lambda_m x) + \Phi_2 \cos(2\delta_n y)$$
$$+\Phi_3 \sin(\lambda_m x)\sin(\delta_n y) + \frac{1}{2}P_x y^2 + \frac{1}{2}P_y x^2 \quad (31)$$

where P_x and P_y are applied in-plane load in x and y directions and

$$\Phi_1 = \frac{\delta_n^2}{32\tilde{A}_{11}\lambda_m^2}\tilde{W}(\tilde{W} + 2W^*), \quad \Phi_1 = \frac{\lambda_m^2}{32\tilde{A}_{22}\delta_n^2}\tilde{W}(\tilde{W} + 2W^*),$$
$$\Phi_3 = [\frac{1}{\tilde{A}_{11}\lambda_m^4 + \tilde{A}_{22}\delta_n^4 + (\tilde{A}_{66} - 2\tilde{A}_{12})\lambda_m^2\delta_n^2}\left(\frac{\delta_n^2}{R_x} + \frac{\lambda_m^2}{R_y}\right)$$
$$-\frac{B_{21}\lambda_m^4 + B_{12}\delta_n^4 + (B_{11} + B_{22} - 2B_{66})\lambda_m^2\delta_n^2}{\tilde{A}_{11}\lambda_m^4 + \tilde{A}_{22}\delta_n^4 + (\tilde{A}_{66} - 2\tilde{A}_{12})\lambda_m^2\delta_n^2}]W$$

Now, Eqs. (29)-(31) can be inserted in Eq.(23) to find the governing equation as:

$$S_1\tilde{W} + S_2\tilde{W}^3 + S_3\tilde{W}^2 W^* + S_4\tilde{W}\left(W^*\right)^2 + S_5 W^* = 0 \quad (32)$$

where S_1 and S_5 are the linear stiffness matrices of perfect and imperfect shells respectively. S_i (i=2, 3, 4) denote nonlinear stiffness matrices. Note that for studying nonlinear stability of doubly-curved shells under lateral pressure let P_x=P_y=0. Also, for studying nonlinear stability of single-curve shells under axial load (P_x), it is crucial to consider q=P_y=0. The nonlinear governing equation has been solved for finding post-buckling curves of the shell based on the variation of P or q versus normalized deflection $\tilde{W}/h$. Here, calculations have been carried out according to below dimensionless factors:

$$K_W = \mathrm{k}_W \frac{\mathrm{a}^4}{D_{11}}, \quad K_p = \mathrm{k}_p \frac{\mathrm{a}^2}{D_{11}} \quad (33)$$

5. Discussion on findings

According to the section, post-buckling of a porous doubly-curved shell modeled via nonlinear imperfect thin shell theory has been studied based upon provided solution approach. The doubly curved shell with stiffeners is shown in Figs.1 and 2. Also, porosity distributions are indicated in Fig.3. The dependency of nonlinear buckling load to the porosity distributions, foundation parameters, dimensionless amplitude, stiffeners, geometrical imperfection and geometrical factors will be discussed. As the first step, post-buckling responses of ideal and imperfect plates have been validated with those reported by Chikh *et al*. (2016) based on functionally graded (FG) plate model, as provided in Table 1. According to the table, buckling loads have been provided for both perfect ($W^*/h = 0$) and imperfect

($W^*/h = 0.1$) plates based on various normalized amplitude. In this research, obtained results based on metal foam material are presented using the below properties:

$$E_2 = 200\ GPa,\ \rho_2 = 7850\ kg/m^3,\ v = 0.33,$$

Influences of pore content (e_0) on the post-buckling properties of curved panel are presented in Fig. 4 at imperfection amplitude of W^*/h=0.1. Uniform pore distribution has been considered. In the case of ideal (perfect) porous doubly-curved panel, the load at $\widetilde{W}/h = 0$is critical buckling load. However, in the case of imperfect porous curved panel ($W^*/h \neq 0$), the critical buckling load does not exist, because the shell has an initial deflection. It must be pointed out that the buckling load becomes greater by increasing in normalized amplitude. The reason is intrinsic stiffening impact raised from geometric nonlinearity. Decreasing effect of porosities on mechanical properties of the shell is obviously observable from this graph. In fact, the effective stiffness of the porous doubly-curved panel may be prominently diminished via adding a small amount of pores to matrix material. Thus, post-buckling loads reduce by increasing in porosity content.

Fig. 5 presents the variation of pressure-deflection curves of a doubly-curved shell under transverse loading when a/h=50 and $W^*/h = 0.1$ based on various values of porosity coefficient. This figure shows that with the increment of dimensionless deflection, obtained pressure becomes larger regardless of the value of porosity coefficient. At a prescribed value of dimensionless deflection, increase of porosity coefficient leads to smaller pressures. This means that porosities make the shell structure more flexible. This observation is valid for both perfect and imperfect doubly-curved shells.

In Figs. 6 and 7, the load-deflection and pressure-deflection curves have been illustrated based on the types of porosity distribution at a fixed value of porosity coefficient e_0=0.5. Derived findings indicate that the curved shell with non-uniform pore distributions have higher nonlinear buckling load and pressure than uniform pore distributions. Such a fact reveals that the curved shell with symmetrically dispersed pores may introduce the higher shell stiffness together with the better mechanical performances. Indeed, pore distribution has a notable impact on buckling behaviors and may be incorporated in stability studies of curved shells. According to previous discussions, the material properties of porous curved shells are un-varied along the thickness in the case uniform pore distributions. Whereas, the material properties become maximum at upper and lower surfaces in the case of non-uniform pore distributions.

Fig.8 indicates the post-bucking curves of the porous shell with and without the effect of stiffeners. Uniform porosity distribution with e_0=0.2 is considered. Geometrical parameters of the stiffener are selected as s_x=0.4a, z_x=0.01a, h_x=0.01h, d_x=0.005a. This figure shows that stiffened curved shells have enhanced load carrying capacities since they are reinforced by a system of stiffeners. Therefore, post-buckling loads of stiffened curved shells are higher than those of curved shells without stiffeners. As stated before, porous curved shells have smaller buckling loads than perfect one. So, their buckling curves can be enhanced by using stiffeners leading to higher buckling loads.

Table 1 Validation of post-buckling loads of ideal and imperfect flat panel for different dimensionless amplitudes (a/R_x=0)

$\widetilde{W}/h$	$W^*/h = 0$		$W^*/h = 0.1$	
	Chikh *et al*. 2016	present	Chikh *et al*. 2016	present
0	0.62411	0.62411	0	0
0.1	0.62627	0.62627	0.31853	0.31853
0.2	0.63274	0.63274	0.43334	0.43334
0.3	0.64354	0.64354	0.50047	0.50047

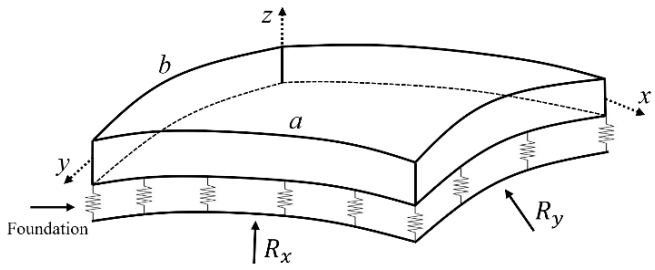

Fig. 1 Geometry of a double-curve shell on elastic foundation

Effects of length-to-thickness ratio (a/h) on post-buckling behaviors of porous curved panel have been plotted in Fig.9. Two cases of geometrically ideal (perfect) and imperfect shells have been supposed. It is obvious that shells are less rigid at greater values for a/h. Accordingly, derived post-buckling load becomes lower via enlargement of a/h at prescribed normalized amplitudes ($\widetilde{W}/h$). Also, calculated post-buckling loads for various values of a/h rely on the magnitude of normalized deflection. For smaller a/h, post-buckling load increases with a higher slope according to normalized deflection than higher length-to-thickness ratio or thinner shells. Such observation is due to more stiffness of the plate at low values of a/h.

Fig. 10 indicates the variation of post-buckling load of a porous curved panel versus normalized amplitude for various linear (K_W), shear (K_P) foundation factors. It must be pointed out that the shear layer gives continuous interactions with the porous doubly-curved panel, whereas linear layer gives discontinuous interactions with the plate. Growth of foundation factors results in greater nonlinear buckling load via improving the bending rigidity of porous doubly-curved panel.

Geometrical imperfection (W^*/h) effect on post-buckling behavior of porous curved panel has been illustrated in Fig.11. IT may be observed that the initial deflection of shell has notable influences on the post-buckling load-deflection path. Based on previous discussion, the critical buckling load vanishes by considering plate initial deflection. In fact, for the case of perfect structure ($W^*/h = 0$), the shell has critical buckling. Next, shell buckling capacity improves by the increase of normalized deflection. However, for the case of

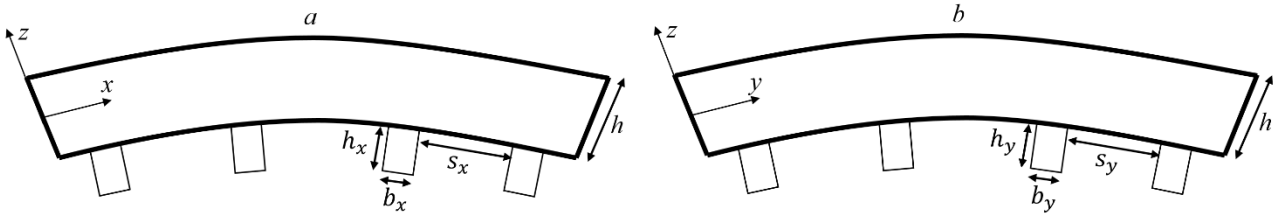

Fig. 2 Side views of a double-curve shell with stiffeners

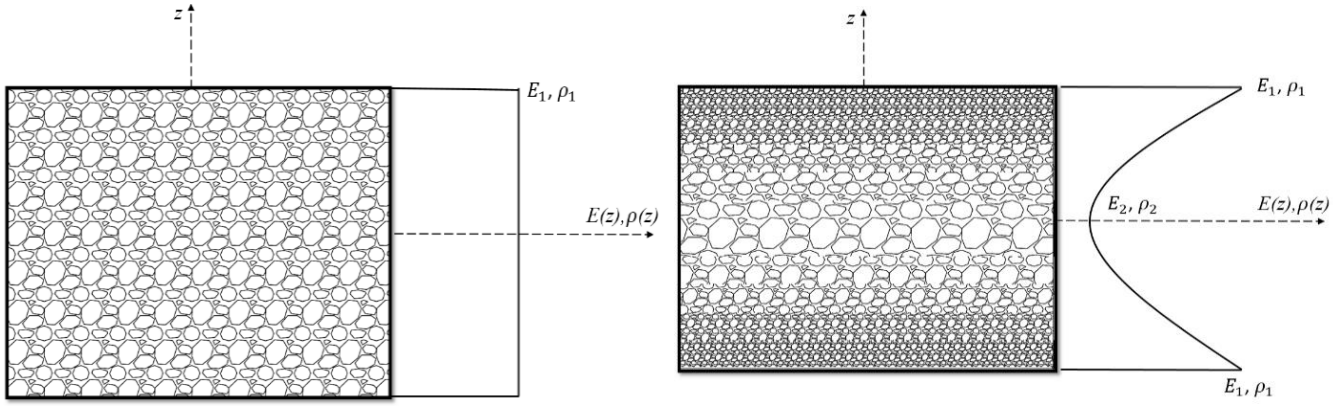

(a) Uniform (b) Non-uniform

Fig. 3 Two types of porosity distributions inside metal foam

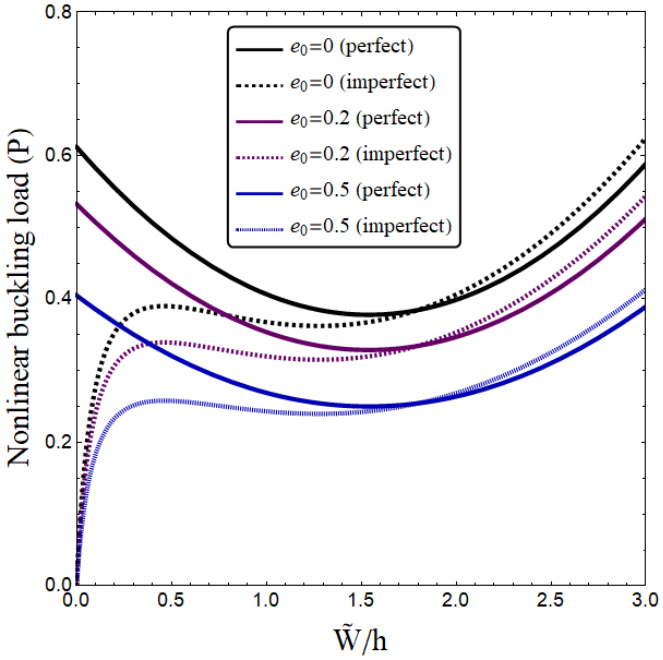

Fig. 4 Nonlinear buckling load versus normalized deflection of the shell for various porosity coefficients (a/h=50, R/a=4, W*/h=0.1)

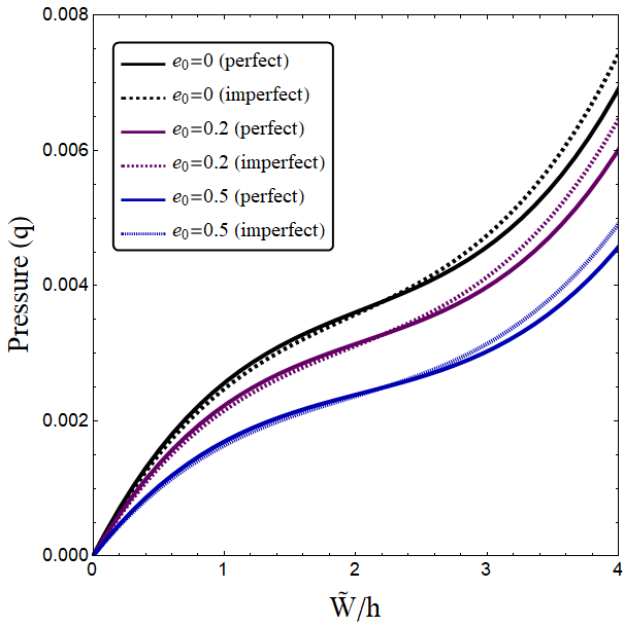

Fig. 5 Pressure-deflection curves of doubly-curved shell for various porosity coefficients (a/h=50, R/a=4, W*/h=0.1)

imperfect structure ($W^*/h \neq 0$), there is no buckling load before the initial situation of porous curved panel. Thus, the buckling load is zero at the starting point for imperfect plates. After that, greater amplitudes of shells need stronger compressive load. Finally, it may be concluded that pot-buckling curves of perfect and imperfect shells become closer to each other at large values for normalized amplitude.

6. Conclusions

This article analyzed post-buckling behaviors of imperfect and porous doubly-curved shells via stablishing a nonlinear shell formulation in which stiffeners effects are involved. Both uniform and non-uniform pore distributions were considered. Obtained finding in this research are presented as follows.

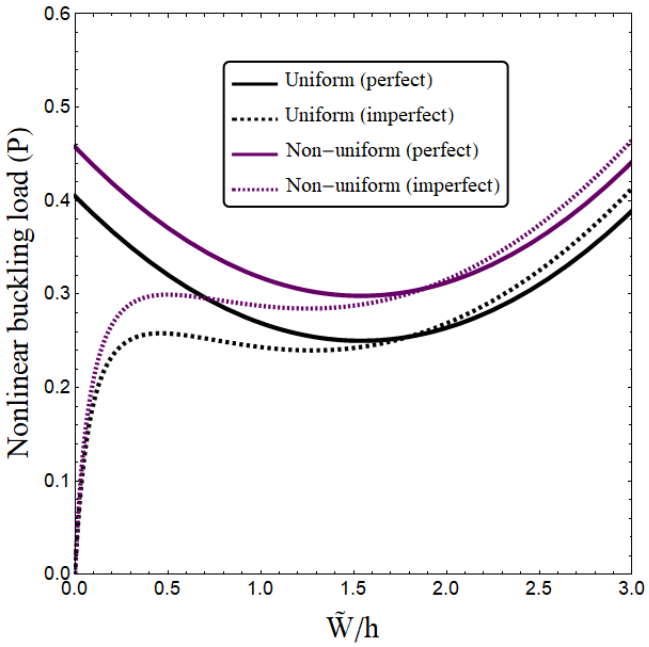

Fig. 6 Nonlinear buckling load versus normalized deflection of the shell for various porosity distributions (a/h=50, R/a=4, W*/h=0.1, e_0=0.5)

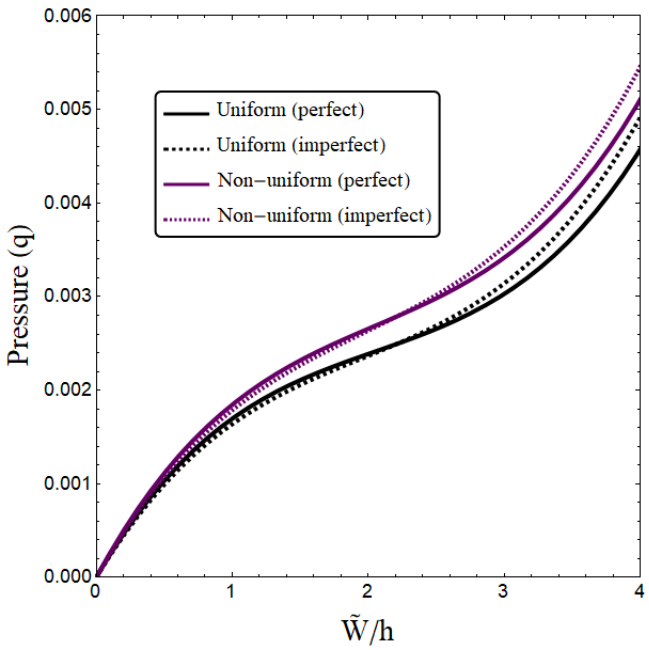

Fig. 7 Pressure-deflection curves of doubly-curved shell for various porosity distributions (a/h=50, R/a=4, W*/h=0.1, e_0=0.5)

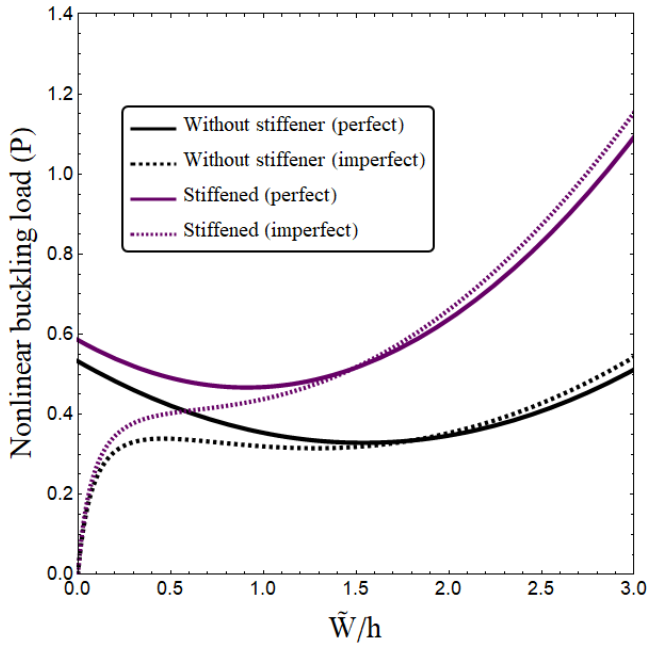

Fig. 8 Nonlinear buckling load versus normalized deflection of porous shell with and without stiffeners (a/h=50, R/a=4, W*/h=0.1, e_0=0.2, s_x=0.4a, z_x=0.01a, h_x=0.01h, d_x=0.005a)

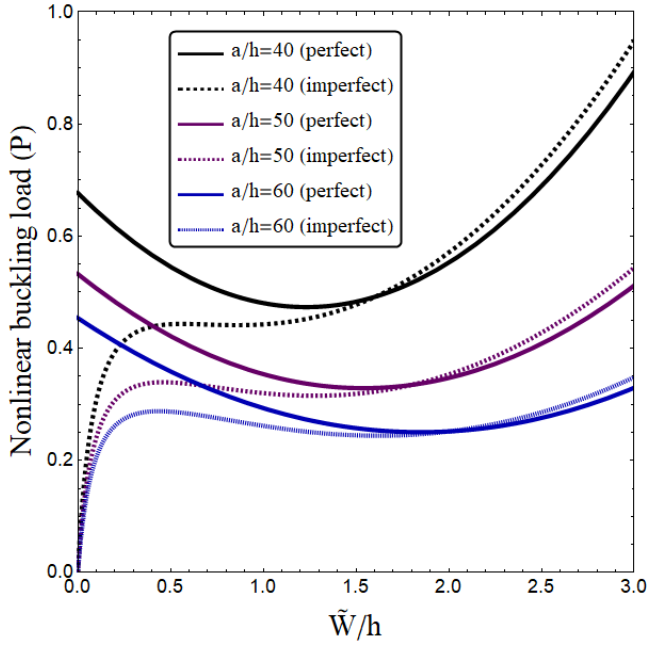

Fig. 9 Nonlinear buckling load versus normalized deflection of porous shell based on various length-to-thickness rations (R/a=4, W*/h=0.1, e_0=0.2)

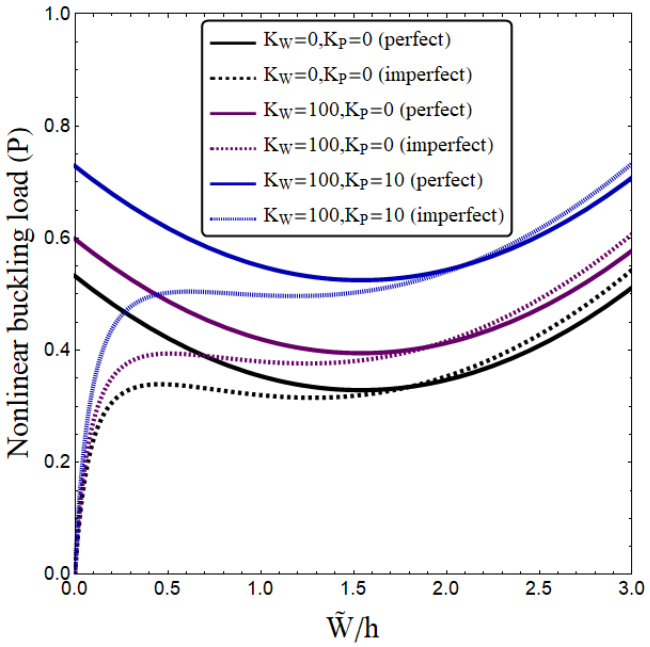

Fig. 10 Nonlinear buckling load versus normalized deflection of porous shell based on various length-to-thickness rations (a/h=50, R/a=4, W*/h=0.1, e_0=0.2)

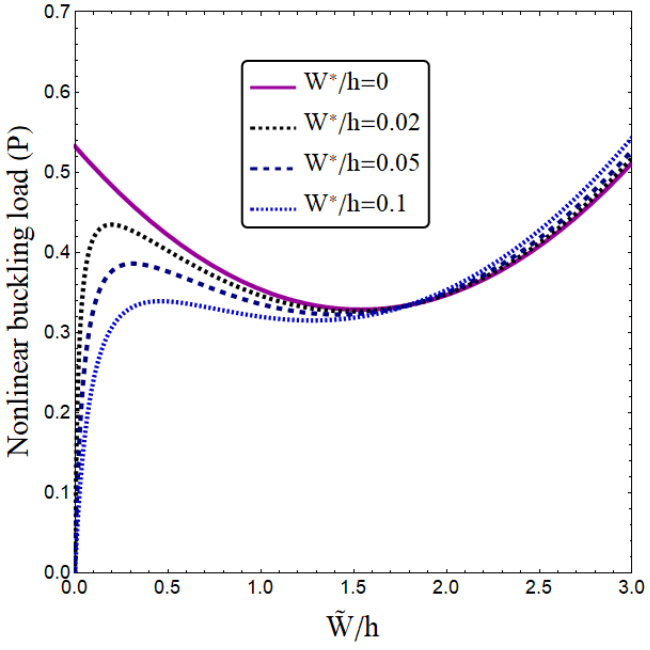

Fig. 11 Nonlinear buckling load versus normalized deflection of porous shell based on various length-to-thickness rations (a/h=50, R/a=4, e_0=0.2)

- The most important observation was that increasing pore amount yields lower buckling loads for all types of pore distributions. It means that adding the amount of pores can reduce the shell stiffness and decrease its post-buckling behavior.
- Moreover, uniform pore distribution provided lower post-buckling loads than non-uniform distribution. This is due to larger amount of pores based on uniform dispersion.
- An important finding was that as the magnitude of imperfection is greater, the post-buckling load is lower.
- Stiffened curved shells have enhanced load carrying capacities since they are reinforced by a system of stiffeners.

Acknowledgments

The first and second authors would like to thank FPQ (Fidar project Qaem) for providing the fruitful and useful help.

References

Abualnour, M., Chikh, A., Hebali, H., Kaci, A., Tounsi, A., Bousahla, A. A. and Tounsi, A. (2019), "Thermomechanical analysis of antisymmetric laminated reinforced composite plates using a new four variable trigonometric refined plate theory," *Comput. Concrete*, **24**(6), 489-498. https://doi.org/10.12989/cac.2019.24.6.489.

Abdelaziz, H. H., Meziane, M. A. A., Bousahla, A. A., Tounsi, A., Mahmoud, S. R. and Alwabli, A. S. (2017), "An efficient hyperbolic shear deformation theory for bending, buckling and free vibration of FGM sandwich plates with various boundary conditions," *Steel Compos. Struct.*, **25**(6), 693-704. https://doi.org/10.12989/scs.2017.25.6.693.

Achouri, F., Benyoucef, S., Bourada, F., Bouiadjra, R. B. and Tounsi, A. (2019), "Robust quasi 3D computational model for mechanical response of FG thick sandwich plate", *Struct. Eng. Mech.*, **70**(5), 571-589. https://doi.org/10.12989/sem.2019.70.5.571.

Adda Bedia, W.A., Houari, M. S. A., Bessaim, A., Bousahla, A. A., Tounsi, A., Saeed, T. and Alhodaly, M. S. (2019), "A New Hyperbolic Two-Unknown Beam Model for Bending and Buckling Analysis of a Nonlocal Strain Gradient Nanobeams", *J. Nano Res.*, **57**, 175-191. https://doi.org/10.4028/www.scientific.net/JNanoR.57.175.

Addou, F. Y., Meradjah, M., Bousahla, A. A., Benachour, A., Bourada, F., Tounsi, A. and Mahmoud, S. R. (2019), "Influences of porosity on dynamic response of FG plates resting on Winkler/Pasternak/Kerr foundation using quasi 3D HSDT", *Comput. Concrete*, **24**(4), 347-367. https://doi.org/10.12989/cac.2019.24.4.347.

Ahmed, R. A., Fenjan, R. M. and Faleh, N. M. (2019), "Analyzing post-buckling behavior of continuously graded FG nanobeams with geometrical imperfections", *Geomech. Eng.*, **17**(2), 175-180. https://doi.org/10.12989/gae.2019.17.2.175.

Aissani, K., Bouiadjra, M.B., Ahouel, M. and Tounsi, A. (2015), "A new nonlocal hyperbolic shear deformation theory for nanobeams embedded in an elastic medium", *Struct. Eng. Mech.*, **55**(4), 743-763. https://doi.org/10.12989/sem.2015.55.4.743.

Alimirzaei, S., Mohammadimehr, M. and Tounsi, A. (2019), "Nonlinear analysis of viscoelastic micro-composite beam with geometrical imperfection using FEM: MSGT electro-magneto-elastic bending, buckling and vibration solutions", *Struct. Eng. Mech.*, **71**(5), 485-502. http://dx.doi.org/10.12989/sem.2019.71.5.485.

Al-Maliki, A. F., Faleh, N. M. and Alasadi, A. A. (2019), "Finite element formulation and vibration of nonlocal refined metal foam beams with symmetric and non-symmetric porosities", *Struct. Monitor. Maintenance*, **6**(2), 147-159. https://doi.org/10.12989/smm.2019.6.2.147.

Asghar, S., Naeem, M. N., Hussain, M., Taj, M. and Tounsi, A. (2020), "Prediction and assessment of nonlocal natural frequencies of DWCNTs: Vibration analysis", *Comput. Concrete*, **25**(2), 133-144. https://doi.org/10.12989/cac.2020.25.2.133.

Attia, A., Bousahla, A.A., Tounsi, A., Mahmoud, S.R. and Alwabli, A.S. (2018), "A refined four variable plate theory for thermoelastic analysis of FGM plates resting on variable elastic foundations", *Struct. Eng. Mech.*, **65**(4), 453-464. https://doi.org/10.12989/sem.2018.65.4.453.

Atmane, H.A., Tounsi, A., Bernard, F .and Mahmoud, S.R. (2015), "A computational shear displacement model for vibrational analysis of functionally graded beams with porosities", *Steel Compos. Struct.*, **19**(2), 369-384. https://doi.org/10.12989/scs.2015.19.2.369.

Azimi, M., Mirjavadi, S.S., Shafiei, N. and Hamouda, A.M.S. (2017), "Thermo-mechanical vibration of rotating axially functionally graded nonlocal Timoshenko beam", *Appl. Phys. A*, **123**(1), 104. http://dx.doi.org/10.1007/s00339-017-0772-1.

Azimi, M., Mirjavadi, S. S., Shafiei, N., Hamouda, A. M. S. and Davari, E. (2018), "Vibration of rotating functionally graded Timoshenko nano-beams with nonlinear thermal distribution", *Mech. Adv. Mater. Struct.*, **25**(6), 467-480. https://doi.org/10.1080/15376494.2017.1285455.

Balubaid, M., Tounsi, A., Dakhel, B. and Mahmoud, S. R. (2019), "Free vibration investigation of FG nanoscale plate using nonlocal two variables integral refined plate theory", *Comput. Concrete*, **24**(6), 579-586. https://doi.org/10.12989/cac.2019.24.6.579.

Barati, M. R. and Zenkour, A. M. (2018), "Post-buckling analysis of imperfect multi-phase nanocrystalline nanobeams considering nanograins and nanopores surface effects. *Compos. Struct.*, **184**, 497-505. https://doi.org/10.1016/j.compstruct.2017.10.019.

Batou, B., Nebab, M., Bennai, R., Atmane, H. A., Tounsi, A. and Bouremana, M. (2019), "Wave dispersion properties in imperfect sigmoid plates using various HSDTs", *Steel Compos. Struct.*, **33**(5), 699. https://doi.org/10.12989/scs.2019.33.5.699.

Belbachir, N., Draich, K., Bousahla, A. A., Bourada, M., Tounsi, A. and Mohammadimehr, M. (2019), "Bending analysis of anti-symmetric cross-ply laminated plates under nonlinear thermal and mechanical loadings", *Steel Compos. Struct.*, **33**(1), 913-924. https://doi.org/10.12989/scs.2019.33.1.081.

Berghouti, H., Adda Bedia, E. A., Benkhedda, A. and Tounsi, A. (2019), "Vibration analysis of nonlocal porous nanobeams made of functionally graded material", *Adv. Nano Res.*, **7**(5), 351-364. https://doi.org/10.12989/anr.2019.7.5.351.

Bellifa, H., Bakora, A., Tounsi, A., Bousahla, A. A. and Mahmoud, S. R. (2017), "An efficient and simple four variable refined plate theory for buckling analysis of functionally graded plates", *Steel Compos. Struct.*, **25**(3), 257-270. https://doi.org/10.12989/scs.2017.25.3.257.

Berrabah, H. M., Tounsi, A., Semmah, A. and Adda, B. (2013), "Comparison of various refined nonlocal beam theories for bending, vibration and buckling analysis of nanobeams", *Struct. Eng. Mech.,* **48**(3), 351-365. https://doi.org/10.12989/sem.2013.48.3.351.

Boukhlif, Z., Bouremana, M., Bourada, F., Bousahla, A. A., Bourada, M., Tounsi, A. and Al-Osta, M. A. (2019), "A simple quasi-3D HSDT for the dynamics analysis of FG thick plate on elastic foundation", *Steel Compos. Struct.*, **31**(5), 503-516. https://doi.org/10.12989/scs.2019.31.5.503.

Bourada, F., Bousahla, A. A., Bourada, M., Azzaz, A., Zinata, A. and Tounsi, A. (2019), "Dynamic investigation of porous functionally graded beam using a sinusoidal shear deformation theory", *Wind Struct.*, **28**(1), 19-30. https://doi.org/10.12989/was.2019.28.1.019.

Boutaleb, S., Benrahou, K. H., Bakora, A., Algarni, A., Bousahla, A. A., Tounsi, A., Tounsi, A. and Mahmoud, S. R. (2019), "Dynamic Analysis of nanosize FG rectangular plates based on simple nonlocal quasi 3D HSDT", *Adv. Nano Res.*, **7**(3), 189-206. http://dx.doi.org/10.12989/anr.2019.7.3.191.

Boulefrakh, L., Hebali, H., Chikh, A., Bousahla, A. A., Tounsi, A. and Mahmoud, S. R. (2019), "The effect of parameters of visco-Pasternak foundation on the bending and vibration properties of a thick FG plate", *Geomech. Eng.*, **18**(2), 161-178. https://doi.org/10.12989/gae.2019.18.2.161.

Chaabane, L. A., Bourada, F., Sekkal, M., Zerouati, S., Zaoui, F. Z., Tounsi, A., Bousahla, A. A. and Tounsi, A. (2019), "Analytical study of bending and free vibration responses of functionally graded beams resting on elastic foundation", *Struct. Eng. Mech.*, **71**(2), 185-196. https://doi.org/10.12989/sem.2019.71.2.185.

Chen, D., Yang, J. and Kitipornchai, S. (2015), "Elastic buckling and static bending of shear deformable functionally graded porous beam", *Compos. Struct.*, **133**, 54-61. https://doi.org/10.1016/j.compstruct.2015.07.052.

Chen, D., Kitipornchai, S. and Yang, J. (2016), "Nonlinear free vibration of shear deformable sandwich beam with a functionally graded porous core", *Thin-Walled Struct.*, **107**, 39-48. https://doi.org/10.1016/j.tws.2016.05.025.

Chikh, A., Bakora, A., Heireche, H., Houari, M. S. A., Tounsi, A. and Bedia, E.A. (2016), "Thermo-mechanical postbuckling of symmetric S-FGM plates resting on Pasternak elastic foundations using hyperbolic shear deformation theory", *Struct. Eng. Mech.*, **57**(4), 617-639. https://doi.org/10.12989/sem.2016.57.4.617.

Draiche, K., Bousahla, A. A., Tounsi, A., Alwabli, A. S., Tounsi, A. and Mahmoud, S. R. (2019), "Static analysis of laminated reinforced composite plates using a simple first-order shear deformation theory", *Comput. Concrete*, **24**(4), 369-378. https://doi.org/10.12989/cac.2019.24.4.369.

Draoui, A., Zidour, M., Tounsi, A. and Adim, B. (2019), "Static and dynamic behavior of nanotubes-reinforced sandwich plates using (FSDT)", *J. Nano Res.*, **57**, 117-135. https://doi.org/10.4028/www.scientific.net/JNanoR.57.117.

Duc, N. D., Cong, P. H. and Quang, V. D. (2016), "Thermal stability of eccentrically stiffened FGM plate on elastic foundation based on Reddy's third-order shear deformation plate theory", *J. Therm. Stresses*, **39**(7), 772-794. https://doi.org/10.1080/01495739.2016.1188638.

Duc, N. D. and Quan, T. Q. (2014), "Transient responses of functionally graded double curved shallow shells with temperature-dependent material properties in thermal environment", *European J. Mech. A/Solids*, **47**, 101-123. https://doi.org/10.1016/j.euromechsol.2014.03.002.

Fenjan, R. M., Ahmed, R. A., Alasadi, A. A. and Faleh, N. M. (2019), "Nonlocal strain gradient thermal vibration analysis of double-coupled metal foam plate system with uniform and non-uniform porosities", *Coupled Syst. Mech.*, **8**(3), 247-257. https://doi.org/10.12989/csm.2019.8.3.247.

Hussain, M., Naeem, M. N., Tounsi, A. and Taj, M. (2019), "Nonlocal effect on the vibration of armchair and zigzag SWCNTs with bending rigidity", *Adv. Nano Res.*, **7**(6), 431-442. https://doi.org/10.12989/anr.2019.7.6.431.

Hellal, H., Bourada, M., Hebali, H., Bourada, F., Tounsi, A., Bousahla, A. A. and Mahmoud, S. R. (2019), "Dynamic and stability analysis of functionally graded material sandwich plates in hygro-thermal environment using a simple higher shear deformation theory", *J. Sandwich Struct. Mater*. https://doi.org/10.1177/1099636219845841.

Kaddari, M., Kaci, A., Bousahla, A. A., Tounsi, A., Bourada, F., Tounsi, A., Adda Bedia, E.A. and Al-Osta, M.A. (2020), "A study on the structural behaviour of functionally graded porous plates on elastic foundation using a new quasi-3D model: Bending and Free vibration analysis", *Comput. Concrete*, **25**(1), 37-57. https://doi.org/10.12989/cac.2020.25.1.037.

Khiloun, M., Bousahla, A. A., Kaci, A., Bessaim, A., Tounsi, A. and Mahmoud, S. R. (2019), "Analytical modeling of bending and vibration of thick advanced composite plates using a four-variable quasi 3D HSDT", *Eng. Comput.,* https://doi.org/10.1007/s00366-019-00732-1.

Li, H., Pang, F., Gong, Q. and Teng, Y. (2019), "Free vibration analysis of axisymmetric functionally graded doubly-curved shells with un-uniform thickness distribution based on Ritz method", *Compos. Struct.*, **225**, 111145. https://doi.org/10.1016/j.compstruct.2019.111145.

Mahmoudi, A., Benyoucef, S., Tounsi, A., Benachour, A., Adda Bedia, E. A. and Mahmoud, S. R. (2019), "A refined quasi-3D shear deformation theory for thermo-mechanical behavior of functionally graded sandwich plates on elastic foundations", *J. Sandwich Struct. Mater.*, **21**(6), 1906-1929. https://doi.org/10.1177/1099636217727577.

Mechab, I., Mechab, B., Benaissa, S., Serier, B and Bouiadjra, B. B. (2016), "Free vibration analysis of FGM nanoplate with porosities resting on Winkler Pasternak elastic foundations based on two-variable refined plate theories", *J. Brazilian Soc. Mech. Sci. Eng.*, **38**(8), 2193-2211. https://doi.org/10.1007/s40430-015-0482-6.

Medani, M., Benahmed, A., Zidour, M., Heireche, H., Tounsi, A., Bousahla, A. A. and Mahmoud, S. R. (2019), "Static and dynamic behavior of (FG-CNT) reinforced porous sandwich plate using energy principle", *Steel Compos. Struct.*, **32**(5), 595-610. https://doi.org/10.12989/scs.2019.32.5.595.

Meksi, R., Benyoucef, S., Mahmoudi, A., Tounsi, A., Adda Bedia, E. A. and Mahmoud, S. R. (2019), "An analytical solution for bending, buckling and vibration responses of FGM sandwich plates", *J. Sandwich Struct. Mater.*, **21**(2), 727-757. https://doi.org/10.1177%2F1099636217698443.

Mirjavadi, S. S., Rabby, S., Shafiei, N., Afshari, B. M. and Kazemi, M. (2017), "On size-dependent free vibration and thermal buckling of axially functionally graded nanobeams in thermal environment", *Appl. Phys. A*, **123**(5), 315.

Mirjavadi, S. S., Afshari, B. M., Shafiei, N., Hamouda, A.M.S. and Kazemi, M. (2017), "Thermal vibration of two-dimensional functionally graded (2D-FG) porous Timoshenko nanobeams", *Steel Compos. Struct*, **25**(4), 415-426.

Mirjavadi, S. S., Afshari, B. M., Barati, M. R. and Hamouda, A. M. S. (2018), "Strain gradient based dynamic response analysis of heterogeneous cylindrical microshells with porosities under a moving load", *Mater. Res. Express*, **6**(3), 035029.

Mirjavadi, S. S., Afshari, B. M., Khezel, M., Shafiei, N., Rabby, S. and Kordnejad, M. (2018), "Nonlinear vibration and buckling of functionally graded porous nanoscaled beams", *J. Brazilian Soc. Mech. Sci. Eng.*, **40**(7), 352.

Mirjavadi, S. S., Forsat, M., Hamouda, A. M. S. and Barati, M. R. (2019), "Dynamic response of functionally graded graphene nanoplatelet reinforced shells with porosity distributions under transverse dynamic loads", *Mater. Res. Exp.*, **6**(7), 075045.

Mirjavadi, S. S., Forsat, M., Nikookar, M., Barati, M. R. and Hamouda, A. M. S. (2019), "Nonlinear forced vibrations of sandwich smart nanobeams with two-phase piezo-magnetic face sheets", *European Physical J. Plus*, **134**(10), 508.

Mirjavadi, S. S., Afshari, B. M., Barati, M. R. and Hamouda, A. M. S. (2019), "Transient response of porous FG nanoplates subjected to various pulse loads based on nonlocal stress-strain gradient theory", *European J. Mech. A/Solids*, **74**, 210-220.

Mirjavadi, S. S., Afshari, B. M., Barati, M. R. and Hamouda, A. M. S. (2019), "Nonlinear free and forced vibrations of graphene nanoplatelet reinforced microbeams with geometrical imperfection", *Microsyst. Technol.*, **25**, 3137–3150.

Mirjavadi, S. S., Forsat, M., Barati, M. R., Abdella, G. M., Hamouda, A. M. S., Afshari, B. M. and Rabby, S. (2019), "Post-buckling analysis of piezo-magnetic nanobeams with geometrical imperfection and different piezoelectric contents", *Microsyst. Technol.*, **25**(9), 3477-3488.

Mirjavadi, S. S., Forsat, M., Barati, M. R., Abdella, G. M., Afshari, B. M., Hamouda, A. M. S. and Rabby, S. (2019), "Dynamic response of metal foam FG porous cylindrical micro-shells due to moving loads with strain gradient size-dependency", *European Phys. J. Plus*, **134**(5), 214.

Nebab, M., Atmane, H. A., Bennai, R. and Tahar, B. (2019), "Effect of nonlinear elastic foundations on dynamic behavior of FG plates using four-unknown plate theory", *Earthq. Struct.*, **17**(5), 447-462. https://doi.org/10.12989/eas.2019.17.5.447.

Sahla, M., Saidi, H., Draiche, K., Bousahla, A. A., Bourada, F. and Tounsi, A. (2019), "Free vibration analysis of angle-ply laminated composite and soft core sandwich plates", *Steel Compos. Struct.*, **33**(5), 663-679. https://doi.org/10.12989/scs.2019.33.5.663.

Sahu, S. A., Singhal, A. and Chaudhary, S. (2018), "Surface wave propagation in functionally graded piezoelectric material: An analytical solution", *J. Intelligent Mater. Syst. Struct.*, **29**(3), 423-437. https://doi.org/10.1177/1045389X17708047.

Semmah, A., Heireche, H., Bousahla, A.A., Tounsi, A. (2019), "Thermal buckling analysis of SWBNNT on Winkler foundation by non local FSDT", *Adv. Nano Res*., **7**(2), 89-98.

Shafiei, N., Mirjavadi, S. S., Afshari, B. M., Rabby, S. and Hamouda, A. M. S. (2017)", Nonlinear thermal buckling of axially functionally graded micro and nanobeams", *Compos. Struct*., 168, 428-439.

Tlidji, Y., Zidour, M., Draiche, K., Safa, A., Bourada, M., Tounsi, A., Bousahla, A.A. and Mahmoud, S.R. (2019), "Vibration analysis of different material distributions of functionally graded microbeam", *Struct. Eng. Mech.*, **69**(6), 637-649.

Trinh, M. C., Nguyen, D. D. and Kim, S. E. (2019), "Effects of porosity and thermomechanical loading on free vibration and nonlinear dynamic response of functionally graded sandwich shells with double curvature", *Aerosp. Sci. Technol.*, **87**, 119-132. https://doi.org/10.1016/j.ast.2019.02.010.

Tounsi, A., Al-Dulaijan, S.U., Al-Osta, M.A., Chikh, A., Al-Zahrani, M. M., Sharif, A. and Tounsi, A. (2020), "A four variable trigonometric integral plate theory for hygro-thermo-mechanical bending analysis of AFG ceramic-metal plates resting on a two-parameter elastic foundation", *Steel Compos. Struct.*, **34**(4), 511-524.

Wattanasakulpong, N and Ungbhakorn, V. (2014), "Linear and nonlinear vibration analysis of elastically restrained ends FGM beams with porosities", *Aerosp. Sci. Technol.*, **32**(1), 111-120. https://doi.org/10.1016/j.ast.2013.12.002.

Yahiaoui, M., Tounsi, A., Fahsi, B., Bouiadjra, R.B. and Benyoucef, S. (2018), "The role of micromechanical models in the mechanical response of elastic foundation FG sandwich thick beams", *Struct. Eng. Mech.*, **68**(1), 053. https://doi.org/10.12989/sem.2018.68.1.053.

Zare Jouneghani, F., Dimitri, R., Bacciocchi, M. and Tornabene, F. (2017), "Free vibration analysis of functionally graded porous doubly-curved shells based on the first-order shear deformation theory", *Appl. Sci.*, **7**(12), 1252. https://doi.org/10.3390/app7121252.

Zarga, D., Tounsi, A., Bousahla, A. A., Bourada, F. and Mahmoud, S.R. (2019), "Thermomechanical bending study for functionally graded sandwich plates using a simple quasi-3D shear deformation theory", *Steel Compos. Struct.*, **32**(3), 389-410. https://doi.org/10.12989/scs.2019.32.3.389.

Zaoui, F. Z., Ouinas, D. and Tounsi, A. (2019), "New 2D and quasi-3D shear deformation theories for free vibration of functionally graded plates on elastic foundations", *Compos. Part B*, **159**, 231-247. https://doi.org/10.1016/j.compositesb.2018.09.051.

Zhao, J., Xie, F., Wang, A., Shuai, C., Tang, J. and Wang, Q.

(2019), "A unified solution for the vibration analysis of functionally graded porous (FGP) shallow shells with general boundary conditions", *Compos. Part B Eng.*, **156**, 406-424. https://doi.org/10.1016/j.compositesb.2018.08.115.

Zine, A., Tounsi, A., Draiche, K., Sekkal, M. and Mahmoud, S. R. (2018), "A novel higher-order shear deformation theory for bending and free vibration analysis of isotropic and multilayered plates and shells", *Steel Compos. Struct.*, **26**(2), 125-137. https://doi.org/10.12989/scs.2018.26.2.125.

CC